Materials and Structures (2023) 56:105
https://doi.org/10.1617/s11527-023-02176-y

RILEM TC 266-MRP: round-robin rheological tests on high performance mortar and concrete with adapted rheology—a comprehensive flow curve analysis

Dimitri Feys · Helena Keller · Khadija El Cheikh · Egor Secrieru · Yannick Vanhove

Received: 17 November 2022 / Accepted: 15 April 2023 / Published online: 5 June 2023

Abstract A comprehensive testing program was carried out to compare the rheological properties of flowable concrete that can be obtained from different rheometers. The results obtained from seven rheometers using vane or similar geometries are discussed. A comprehensive flow curve analysis is undertaken for further comparison of the various rheometers. Partially, large differences could be observed between the results obtained from the different rheometers. However, the device-specific trendlines are shown to have significant correlations with the overall baseline. Two potential causes of differences between results are highlighted: imposition/registration of torque/rotational velocity and discrepancies between the measured material flow behavior in the device and the assumed ideal flow pattern. These differences can stem from a deviation from the perfect concentric cylinders system and bottom and top effects, in which the non-homogeneity of the material enhances these effects. It is shown that these effects are more dependent on mix design and rheological properties than on the testing devices. Also, the influence of extending the measuring procedure on measurement results is shown to affect the measured rheological properties of concrete and mortar. Finally, the paper serves as a comprehensive guide on how to interpret

Chair: Mohammed Sonebi.
Deputy Chair: Dimitri Feys.
TC Members: Sofiane Amziane, Rolands Cepuritis, Chafika Djelal-Dantec, Khadija El Cheikh, Siamak Fakhryee Nejad, Shirin Fataei, Dimitri Feys, Markus Greim, Steffen Grünewald, Michael Haist, Irina Ivanova, Stefan Jacobsen, Helena Keller, Kamal Khayat, Karel Lesage, Laurent Libessart, Julian Link, Dirk Lowke, Viktor Mechtcherine, Ivan Navarrete, Arnaud Perrot, Tilo Proske, Nicolas Roussel, Wolfram Schmidt, Geert de Schutter, Egor Secrieru, Mohammed Sonebi, Yannick Vanhove, Jon E. Wallevik, Ammar Yahia, Jiang Zhu.

D. Feys (✉)
Department of Civil, Architectural and Environmental Engineering, Missouri University of Science and Technology, Rolla, MO 65409, USA
e-mail: feysd@mst.edu

H. Keller
Schleibinger Geräte Teubert U. Greim GmbH, 84428 Buchbach, Germany

K. El Cheikh
Magnel-Vandepitte Laboratory, Department of Structural Engineering and Building Materials, Ghent University, Technologiepark-Zwijnaarde 60, 9052 Ghent, Belgium

E. Secrieru
Engineering and Innovation, HeidelbergCement AG, 69181 Leimen, Germany

Y. Vanhove
ULR 4515-LGCgE, Laboratoire de Génie Civil Et Géo-Environnement, Université d'Artois, 62400 Béthune, France

the rheological data and key factors that have to be considered during the analysis.

Keywords Rheology · Flow curve · Yield stress · Viscosity · Rheometer · Round-Robin test · Flowable concrete

1 Introduction

1.1 General

A concrete rheometer comparison campaign was undertaken at the Universite d'Artois, Bethune, France, in May 2018. It consisted of testing nine different devices, capable of evaluating at least one of the following properties: flow curve, structural build-up or interface characterization. While technically, this campaign is not a Round-Robin test, the authors are convinced that the chosen strategy is the best way to compare different devices. By bringing all rheometers together in one laboratory, and using the same mortar and concrete mixtures, the influence of mixer type, mixing energy and environmental conditions is eliminated when comparing results. In fact, the laboratory was divided into different workstations, depending on the owners of each device, so the work can be considered a Round-Robin test. It just happened that all devices were in the same location. The devices, testing and analysis procedures, combined with the raw data, are presented in [1]. In this contribution, a detailed analysis of the flow curve measurement results from different rheometers is presented. The intention is to deliver guidance to rheologists on how to interpret the data and which factors have to be considered in the analysis.

Several concrete rheometer types are currently available on the market showing different geometries, signal processing and data evaluation. A number of testing campaigns employing such rheometers have been performed in the past in an attempt to discover the differences between the results obtained by testing the same material in different devices [2–4]. Besides, concrete is a complicated material from a rheological point of view, due to the large range of particle sizes, time dependency and variety of forces dominating the behavior [5–9]. Therefore, performing rheological tests requires careful considerations to ensure that reliable data can be retrieved. Measurement errors, caused by ongoing structural breakdown or plug flow, can alter the outcome of the measurement [10]. Radial or vertical particle migration and an insufficiently large sheared zone can invalidate the measurements [11, 12]. The following section discusses the occurrence and consequences of such artefacts.

1.2 Challenges during rheological measurements

Concrete is known to be a thixotropic material due to flocculation and hydration forming an internal structure in the cement paste at rest, which can be broken by shear [13]. To perform a rheological flow curve measurement on a cement-based material, it is necessary to impose a reference state by shearing. Typically, the material is pre-sheared at the highest chosen shear rate of the measurement profile for a sufficiently long time, followed by the flow curve measurement [14]. However, different reference states imposed by altering initial shear rates may lead to different sets of rheological properties [15]. Also, if an equilibrium is not achieved, apparent shear-thickening behavior will be visible if the flow curve is determined by decreasing the shear rate or shear stress over time [16].

Plug flow is the indication of a rigid zone with zero shear rate when performing a rheological measurement in the geometry of a concentric cylinder [17, 18], especially at low rotational velocities [19]. The plug flow forms due to the shear rate profile decreasing from the inner cylinder towards the outer cylinder. This phenomenon does not occur in parallel plates geometry. Indeed, as the shear stress decreases with $1/r^2$, where r is the radial distance from the central axis of the rheometer, the shear stress may fall below the (dynamic) yield stress of the tested cementitious material in a portion of the flow domain. When plug flow forms, the plug radius must be taken into account to recalculate the rheological properties. Otherwise, one would underestimate yield stress and overestimate viscosity [10].

Regarding particle migration, it can invalidate the measurement and is the most difficult artefact to detect, as the measurement output has no specific signature behavior [20]. Particle migration can be induced, for example, by shear or gravity. For concentric cylinders rheometers, the shear rate decreases with increasing r, leading to shear-induced particle migration: particles tend to migrate from the inner (high shear rate region) towards the outer cylinder (low shear rate region), creating a non-homogeneous fluid [6]. Particle migration cannot be excluded or prevented due to the shear rate profile. However, shear-induced particle migration can be minimized by performing short duration measurements and limiting the maximum particle size [11]. As particle migration speed is proportional to particle size squared, concrete is much more susceptible compared to mortar. Further, gravity-induced particle migration is unavoidable either. Migration of the particles takes place once the yield stress is exceeded and the stabilizing force keeping all particles suspended is no longer effective [21]. Similarly, as for shear-induced particle migration, larger particles are more prone to faster migration (sinking). Thus, limiting the duration of the measurement is the best option available. Both phenomena could introduce large errors to the rheological measurements. As a consequence, in extreme cases, the shear-induced particle migration could induce a layer depleted of coarse aggregates near the inner cylinder. This will decrease the apparent rheological properties and could potentially concentrate all shearing in this layer. It can be doubted whether the measurement was performed on a homogeneous cementitious material in that case.

For mixtures with higher thixtotropy, and in relation, higher viscosity, longer pre-shear periods are required to achieve the reference state before the measurement, while mixtures with lower viscosity are more prone to any migration effect [6, 10]. Low rotational velocities, high yield stress and low viscosity also increase the chance for plug flow formation and low thickness of the sheared layer. It is in light of these phenomena that mixtures with different combinations of yield stress, viscosity, and different aggregate size were evaluated.

The vane geometry is an approximation to the classical concentric cylinder geometry and is used for the measurement of non-Newtonian fluids such as cement-based materials. It has the advantage to prevent slip between the concrete and the vane. However, in the case of a low number of blades, the flow profile could deviate from the concentric cylinders assumption. Furthermore, Wallevik has shown that pressure effects in a vane geometry may dominate the measured outcome [22]. Luckily, the pressure effect is proportional to the viscosity of the system.

2 Research significance

When comparing rheometers, two potential causes could induce differences between results. The first cause is the imposition and/or registration of torque and/or rotational velocity [2]. It is typically related to the hardware and software of the device, although it can also be associated with an erroneous calibration factor. The consequence of this is that all results are more or less affected in the same way and will be scaled with a certain factor. This implies that one rheometer will provide systematically higher or lower values compared to another if both are working properly [10]. For this reason, the authors have decided to compare the general trends of all rheometers to a reference value or baseline.

The second cause is based on the different geometries of the devices and thus different flow behaviors during the measurement, compared to the assumed, theoretically perfect flow pattern. These differences can be induced due to a deviation from the perfect concentric cylinders system and bottom and top effects, in which the non-homogeneity of the material enhances these effects.

This paper reports a general comparison of flow curves obtained by means of the rheometers used in the round-robin campaign, a detailed analysis of deviations caused by mix designs or rheological properties, and the indication that extending the measuring procedure duration can have important consequences.

3 Materials

In total, eight mixtures were evaluated for flow curves, consisting of three self-consolidating (self-compacting) concrete (SCC) mixtures, C1 to C3, two flowable concrete mixtures designed for foundation construction, C4 and C5, and three flowable mortar mixtures M1–M3. All concrete mixtures contained a combination of crushed and natural sands and a crushed coarse aggregate with a nominal maximum aggregate size (NMS) of 12 mm, except for concrete 3 that had a NMS of 20 mm. The mortar mixtures had a NMS of 4 mm. The mix designs were adjusted to obtain different ranges of yield stress and viscosity values [1]. Due to the risk of extensive plug flow, potentially invalidating measurements, no conventional vibrated

Table 1 Outcomes of the initial slump flow and V-funnel flow time for the mixtures under investigation

Mixture	Slump flow (MM)	V-Funnel flow time (S)
Concrete (C1)	600	22.0
Concrete (C2)	705	5.0
Concrete (C3)	545	–*
Concrete (C4)	610	19.0
Concrete (C5)	405	–*
Mortar (M1)	735	3.1
Mortar (M2)	600	4.4
Mortar (M3)	565	3.3

*None measurable

concrete mixtures were evaluated. Table 1 summarizes the results of slump flow and V-Funnel flow time. The main induced changes between the studied mix designs are as follows:

- C1 was a standard SCC mixture with an initial slump flow of 600 mm and a V-funnel flow time of 22 s.
- C2 was based on the same mix design as C1, but more dispersing admixture was added, leading to an increase in initial slump flow to 705 mm, and a decrease in V-funnel flow time down to 5 s.
- C3 was an adjusted SCC mix design, with a lower water content targeting a higher viscosity. Its initial slump flow was 545 mm, and the V-funnel flow time could not be measured.
- C4 is a completely different mix design for foundations, made with a lower paste content compared to C1. It has an initial slump flow of 610 mm and a V-funnel flow time of 19 s.
- C5 is an adjustment of C4 by adding more viscosity enhancing agent making the mixture more cohesive. It has an initial slump flow of 403 mm and V-funnel flow time could not be evaluated.
- M1 is a standard mortar from the ready-mix company, displaying an initial slump flow of 735 mm using the standard concrete cone and a V-funnel flow time of 3.1 s.
- M2 was an adjusted version of M1, making the mixture more cohesive by adding more viscosity enhancing agent. It showed an initial slump flow of 660 mm and a V-funnel flow time of 4.4 s.
- M3 was an adjustment of M1, increasing further the amount of viscosity enhancing agent and decreasing the dosage of dispersant. As a result, a slump flow of 565 mm and V-funnel flow time of 3.3 s were measured.

4 Methods

Nine different devices were employed for the flow curve determination and analysis. These are four ICAR rheometers, the Viskomat XL, the eBT-V, the RheoCAD and the ConTec 4SCC rheometer. The ICAR devices and the RheoCAD were equipped with four-blade geometry. On the other side the Viskomat XL and eBT-V were equipped with a six-blade vane geometry. In both cases, the measuring geometries replicate concentric cylinder configurations. The RheoCAD also had a helical inner cylinder, which was used alternatingly with the vane geometry. The 4SCC rheometer either had a mixer-type inner cylinder or a Tattersall Mk-II-inspired version. Details on the rheometers, their operating procedures and the geometries can be found in [1].

To determine the flow curves, a pre-shear and stepwise decreasing rotational velocity profile was imposed. For concrete, the pre-shear duration was 20 s, for mortar, it was extended to 30 s. Each stepwise profile consisted of eight steps of 5 s from maximum to minimum applied rotational velocity, except for the 4SCC rheometer, which only allows six steps and a pre-shear procedure. For the ICAR rheometers, the maximum rotational velocity was 0.5 rps and the minimum was 0.025 rps. Reference [1] describes the procedure followed to ensure the same shear rate for the other rheometers by adjusting the rotational velocities, in an attempt to impose the same reference state in each rheometer. However, for the 4SCC rheometer and the helix in the RheoCAD, no fundamental units could be calculated. Rotational velocities in the 4SCC rheometer were kept the same as for the ICAR, while for the helix, the same rotational velocity profile as for the vane geometry in the RheoCAD was imposed. It should be noted that for ICAR 4, a slightly different testing profile was imposed: the pre-shear was extended to 60 s, and each step had a duration of 10 s. The results for ICAR 4 will be discussed separately in this paper.

To ensure that the results are not influenced by measurement artefacts, the following steps were performed during execution and analysis:

- Determination or verification of zero torque value when the rheometer is empty
- Verification of equilibrium or extreme fluctuations of each step
- Determination of yield stress and plastic viscosity with the Reiner-Riwlin equations
- Correction of the rheological properties when a plug flow occurs
- Verification of the thickness of the sheared zone.

For the 4SCC rheometer which did not allow a transformation to fundamental units with the Reiner-Riwlin equation due to the complexity of the geometry, the first two steps were performed, and the values were reported in relative units as the intercept with the torque axis: G (in A), and the slope of the line: H (in A/rps). Similarly, the results for the RheoCAD with helix impeller are presented in relative units, G and H, in Nm and Nms, respectively.

For each mixture, three flow curves were determined: the first just after delivery of the concrete, at the reference time $t = 0$ min. The second and third curves were measured at 50 min and 80 min after the first flow curve, respectively.

5 Outcomes and discussion

5.1 Baseline determination

To be able to compare the general trends in yield stress and viscosity between the different rheometers, a baseline or reference value was established. As most likely none of the rheometers delivered the exact rheological properties, and as there was no method for the team to determine which rheometer was "closest" to the real values, comparing all devices to one reference device was excluded. Instead, the authors decided to calculate a weighted average value for each test, based on six rheometers: three ICAR rheometers, as the ICAR 4 which followed a different procedure was excluded, the Viskomat XL, the eBT-V and the RheoCAD with vane configuration. The weighted average was based on:

- Number of successful data points for each rheometer
- Number of successful measurements for each test (mixture and time)
- Correlation coefficient of the linear regression between the rheometer values and the baseline
- Removal of outliers.

The determination of the baseline started with all valid tests from the rheometer analyses, without giving an interpretation to the values. Values which did not seem to follow the trend were included in the analysis to remain as impartial as possible. The detailed approach is listed below:

- For each rheometer, the number of valid tests in that device was used as a weighing factor. For the initial step, these values were between 16 for the RheoCAD Vane (RheoCAD-V) and 24 for ICAR 2 and the Viskomat XL. It is worth mentioning that the weighing factors for yield stress and viscosity were considered separately; these factors were identical in the first step.
- Based on the weighing factors, the first set of average values of yield stress and viscosity, for each mixture and each time, 24 in total, were determined.
- The values of each rheometer were plotted against the weighted average to determine the best-fitting linear trendline. Besides, each of the 24 tests had a weighing factor as well, corresponding to the number of rheometers which successfully obtained a value for that test. Initially, these numbers were 4, 5 or 6.
- Based on each trendline for each rheometer and parameter, i.e. yield stress and viscosity, the relative difference, delta relative Δ_r, between a specific rheometer value and the fitted general trendline was determined. For example, a rheometer delivered for a certain test a yield stress value of 80 Pa. The weighted average of the yield stress for that specific test was 50 Pa, and the yield stress trendline had an intercept of 10 Pa and a slope of 1.5 for that specific rheometer. As such, the fitted yield stress value with the trendline is 85 Pa from (10 + 1.5•50) and the relative difference $\Delta_r = -0.1$ (from − 5/50). For all Δ_r's of a rheometer, for yield stress and viscosity values separately, the standard deviation was calculated, and the

outliers, based on a 90% confidence interval, assuming a normal distribution, were determined. These outliers were removed in the next iteration.

- After removal of the outliers, the standard deviation of the Δ_r was recalculated and used as an additional weighing factor for the next iteration step. This is reasoned by the fact that the weighing factor for the rheometers with small Δ_r decreased more with each iteration as more results were removed as outliers, compared to the rheometers with a larger range of Δ_r values.

With the outliers removed, the entire iteration was repeated, adjusting the weight factors every time. New trendlines were determined, Δ_r were re-evaluated, and new outliers were found and removed. After three additional iteration steps, no more outliers were determined, and the weighted average was adjusted a final time. These are the baseline values used for the comparison of the rheometers. Table 2 shows the baseline values for the evaluated mixtures and at different testing times. Based on the slump flow

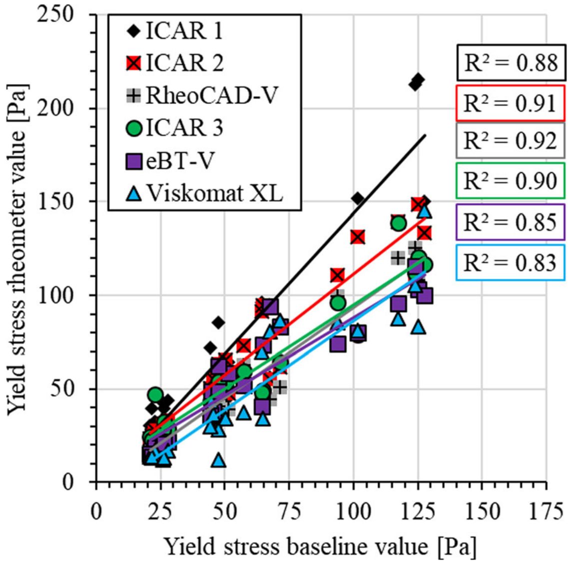

Fig. 1 Comparison between the yield stress values of each rheometer and the calculated baseline. (Color figure online)

Table 2 Calculated baseline values for the investigated mixtures

	Yield stress (Pa)	Plastic viscosity (Pa s)
Concrete (C1)–0 min	67	23
Concrete (C1)–50 min	50	20
Concrete (C1)–80 min	57	25
Concrete (C2)–0 min	46	11
Concrete (C2)–50 min	45	13
Concrete (C2)–80 min	48	18
Concrete (C3)–0 min	51	63
Concrete (C3)–50 min	44	73
Concrete (C3)–80 min	48	90
Concrete (C4)–0 min	71	19
Concrete (C4)–50 min	65	16
Concrete (C4)–80 min	65	28
Concrete (C5)–0 min	125	18
Concrete (C5)–50 min	128	23
Concrete (C5)–80 min	117	24
Mortar (M1)–0 min	23	13
Mortar (M1)–50 min	21	15
Mortar (M1)–80 min	22	15
Mortar (M2)–0 min	28	16
Mortar (M2)–50 min	26	22
Mortar (M2)–80 min	27	22
Mortar (M3)–0 min	124	8
Mortar (M3)–50 min	120	11
Mortar (M3)–80 min	94	12

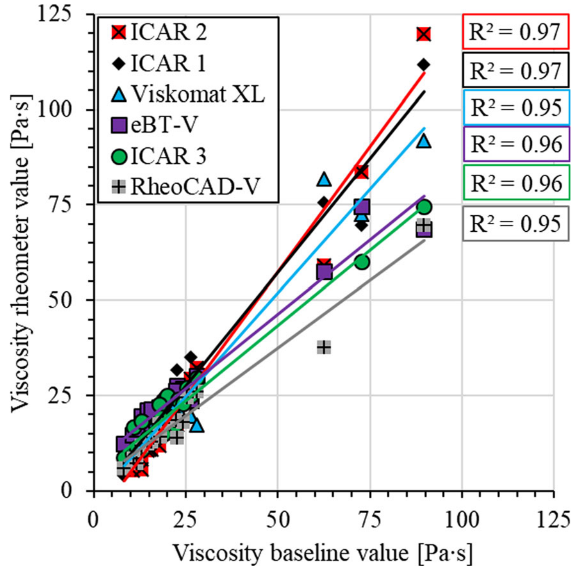

Fig. 2 Comparison between the viscosity values of each rheometer and the calculated baseline. (Color figure online)

measurements, mixtures C2 with 705 mm and M1 with 735 mm, are the most flowable mixtures among the tested concretes and mortars, respectively. This is in line with the values shown in Table 2, as the lowest values of yield stress are observed for these mixtures compared to other concrete or mortar mixtures. This comparison is a quick verification of the followed procedure.

5.2 General correlations between rheometers and baseline

Figures 1 and 2 show the comparison of the yield stress and viscosity, respectively, obtained from the six employed rheometers with the calculated baseline. The figures include all points that were considered to be outliers for the baseline calculation.

The measurement results varied for each rheometer. While the viscosity results are showing very good correlation coefficients greater than 0.95, the results of the yield stress varied showing correlation coefficients in the range of 0.83–0.92, cf. Figs. 1 and 2.

Comparing the intercept points and the slopes of each fitted linear curve, the information about the over- or underestimation of the measured values compared to the baseline can be observed, cf. Fig. 3. All six rheometers used in this testing program showed similar variations compared to the baseline. The closest fitting can be observed for the ICAR 2 and RheoCAD in case of yield stress as well as the Viskomat XL in case of viscosity. The largest estimation could be found for ICAR 1 in case of yield stress and ICAR 2 in case of plastic viscosity. It can be hypothesized that the deviation in the results is primarily dependent on the calibration/registration of the torque and rotational velocity. The purpose of the figures is to provide a general overview of the estimation of yield stress and plastic viscosity. These figures cannot be used to judge the accuracy of the individual rheometers.

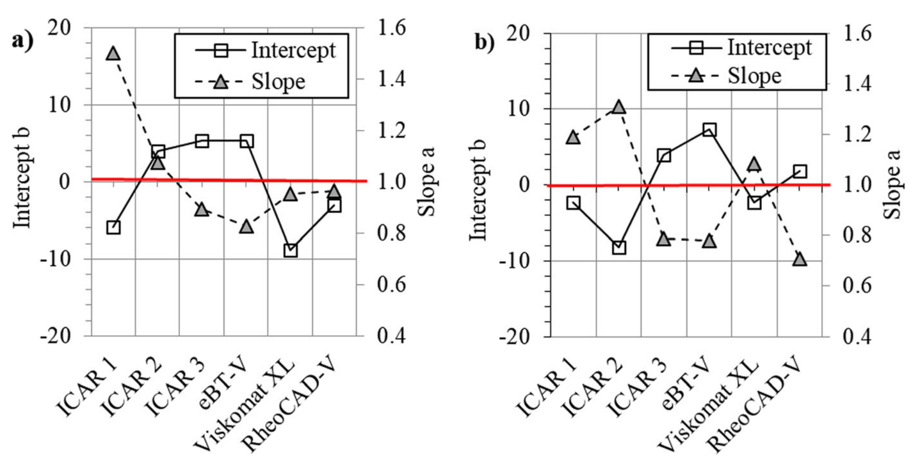

Fig. 3 Comparison of the intercept point and slope of the curves for the rheological parameters yield stress **a** and viscosity **b** related to their weighted average value (red line). (Color figure online)

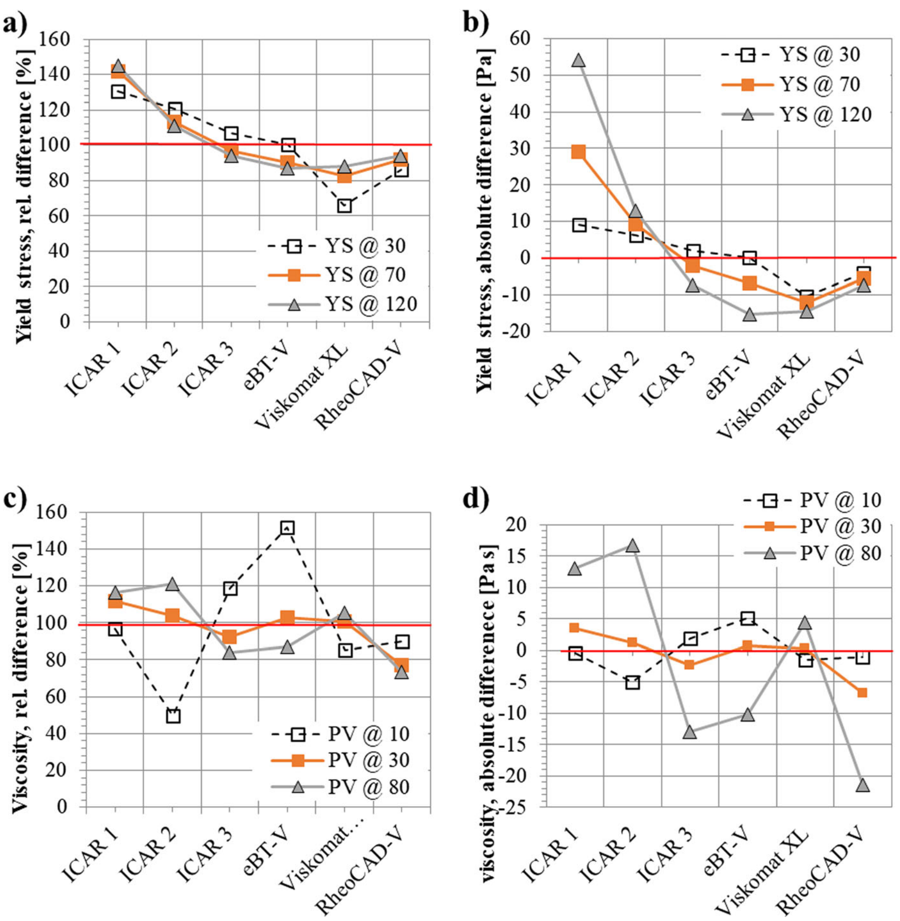

Fig. 4 Relative Δr (left) and absolute Δa (right) difference between the fitted trendline and the baseline for yield stress (top) and viscosity (bottom)

As an example, three different values for the yield stress and the viscosity were taken to represent typical low, medium and high values. Based on the data observed, the rheological values for each rheometer were calculated backwards, cf. Fig. 3. The relative differences Δ_r in % and the absolute differences Δ_a in [Pa] or [Pa·s] are shown in Fig. 4.

For the yield stress, the largest relative difference Δ_r could be observed for the rheometers ICAR 1 for medium and high values and Viskomat XL for low values both in the range of 40%. Compared to this, the best matches could be found for ICAR 3 and eBT-V for low yield stress values. The rheometers ICAR 1 and ICAR 2 provide for all ranges a larger estimation and the rheometers eBT-V, Viskomat XL and RheoCAD a smaller estimation of the yield stress values.

The situation is changing when investigating viscosity. The largest relative differences of about 50% could be found for ICAR 2 and eBT-V at low values and about 20% for ICAR 2 at high values as well as for RheoCAD at medium and high values. The best matches could be observed for ICAR 1 at low viscosity value, ICAR 2 and eBT-V at medium viscosity value and for Viskomat XL for medium and high viscosity values. While the RheoCAD rheometer is showing under-estimation for all viscosity ranges, the measurement results from the rheometers ICAR, eBT-V and Viskomat XL seem to be more affected by the viscosity range.

No significant differences when using a six-bladed vane compared to four-bladed vane could be observed in this round-robin test.

Figure 5 shows adequate correlations for the rheometers which cannot deliver fundamental units,

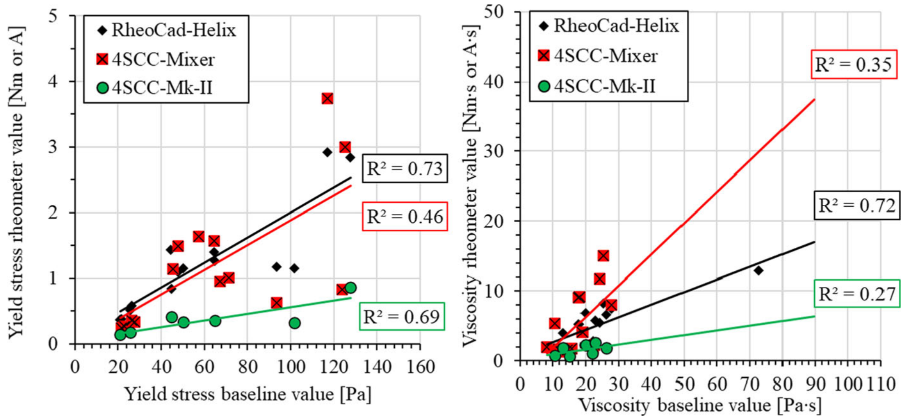

Fig. 5 Comparing of the intercept of the torque-rotational velocity relationship with the torque axis G in [N•m] for the RheoCAD-Helix with helix geometry and [A] for the 4SCC rheometer with the baseline yield stress values (left) and comparing the slope of torque-rotational velocity relationship between H in [Nm•s] for the RheoCAD-Helix and [A•s] for the 4SCC rheometer with the baseline viscosity values (right)

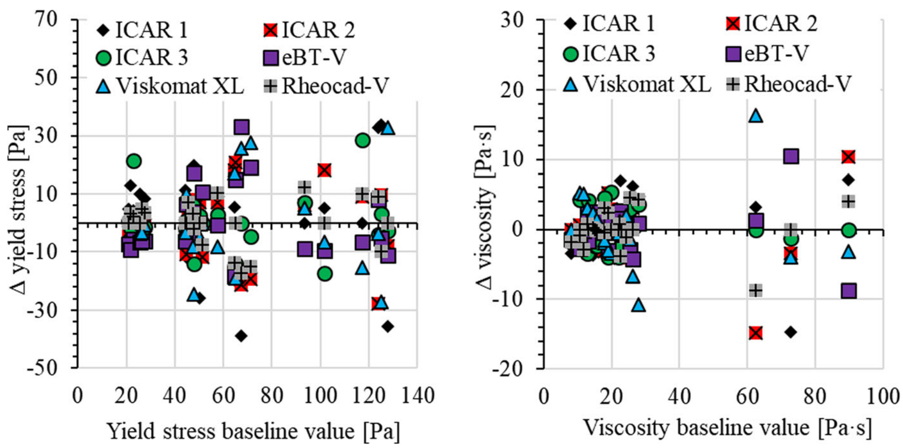

Fig. 6 Scatter around the best fitting line for yield stress (left) and viscosity (right) for each rheometer

with a limited number of test results. The correlation coefficients 0.73 and 0.72 for the RheoCAD with helix, respectively, are still considered adequate. The 4SCC rheometer shows a larger spread in data for the mixer system, and the Mk-II impeller seems to solicit lower relative values of the load cell, which could explain the lower correlation coefficients.

5.3 Investigation of scatter and sensitivity of results to mix designs

In this section, the scatter around the best-fitting lines is discussed. In this regard, for each measurement, the deviation between the data point and the best fitting line is determined. The outliers as determined from the baseline determination, i. e. three for yield stress and two for viscosity, were removed. Figure 6 shows the Δ *yield stress* and Δ *viscosity* for all tests and rheometers used, respectively. The output is a scatter for up to 40 Pa for yield stress and 15 Pa·s for viscosity.

To compare the sensitivity of the measurement to a certain rheometer or a certain mix design, the standard deviation of Δ *yield stress* and Δ *viscosity* was calculated for each rheometer, and separately, for each test. As the average Δ value is zero for each rheometer (since comparing the rheometer with itself) but not for each mixture. The larger the standard deviation, the larger the scatter for that rheometer. A similar approach was followed for each test and mixture, although the averages are not zero. However,

Table 3 Standard deviation on Δ yield stress and Δ viscosity for each rheometer. The first set of values mentioned are the Stdev of the Δ values. The second set of values are the first values divided by the slope of the lines from Fig. 3

Device	Stdev Δ yield stress (Pa)	Stdev Δ viscosity (Pa s)
ICAR 1—VANE	20.4/13.6	4.9/4.1
ICAR 2—VANE	12.2/11.3	4.6/3.5
ICAR 3—VANE	10.9/12.2	3.0/3.8
EBT-V	12.2/14.7	3.5/4.5
VISKOMAT XL	15.2/16.0	5.1/4.7
RHEOCAD—VANE	9.7/10.1	3.4/4.8

Table 4 Averaged standard deviation on Δ yield stress and Δ viscosity for each mixture

Device	Stdev Δyield Stress (Pa)	Stdev Δ viscosity (Pa s)
Concrete (C1)	17.7	4.1
Concrete (C2)	7.5	3.0
Concrete (C3)	11.4	9.3
Concrete (C4)	18.7	5.0
Concrete (C5)	20.7	1.3
Mortar (M1)	7.2	2.1
Mortar (M2)	5.4	2.0
Mortar (M3)	13.9	2.4

it should be noted that the standard deviations for each test were larger than the averages.

Tables 3 and 4 show the standard deviations for each rheometer and each mix design, respectively. The reported values for the mix designs are the average for the three executed tests. The larger the standard deviation (Stdev), the larger the scatter, the more difficult it is for a rheometer to accurately determine the rheological properties of a specific mixture.

The ICAR 1 device shows the largest scatter, cf. Table 3. At the other end are the devices ICAR 3 and the RheoCAD with the smallest deviation. One of the reasons why ICAR 1 shows larger standard deviation values can be traced back to its technical feature to provide systematically larger values. Dividing the Δ *yield stress* values by the slope of the rheometer curve vs. baseline results in adjusted Stdev on Δ *yield stress* between 10.1 and 16.0 Pa, cf. Fig. 1. In case of the Δ *viscosity* parameter values, the adjusted Stdev varies between 3.5 and 4.8 Pa•s, and at the same time alters the order of the rheometers, cf. Fig. 2.

Furthermore, when comparing the range of values in Table 3 with the range of values in Table 4, it can be seen that the scatter is rather dependent on the mix design than on the employed rheometer. It can thus be concluded that, in general, all rheometers which deliver values in fundamental units are affected with the same percentage error throughout the tests. It is thus clear that the scatter on the rheological measurements is primarily induced by the mix design and/or the rheological properties than the rheometers themselves, at least for the devices evaluated.

Figures 7 and 8 summarise the standard deviations of Δ *yield stress* and Δ *viscosity*, for each test separately as a function of the rheological properties.

One could argue that the scatter on the yield stress increases with increasing yield stress and decreases with increasing viscosity values; cf. Fig. 7 left and right. However, especially when not considering test 1 for concrete 1 with a standard deviation of 31 Pa, it seems that C1, C2 and C3 show lower values compared to C4 and C5. Furthermore, the mortars show a lower scatter compared to C4 and C5.

Figure 7 bottom shows the standard deviation of Δ *yield stress* as a function of the ratio of yield stress-to-viscosity. The larger this ratio, the larger the chance for plug flow, and if it occurs, the larger the extent of the plug flow. Smaller flow domains can lead to lower

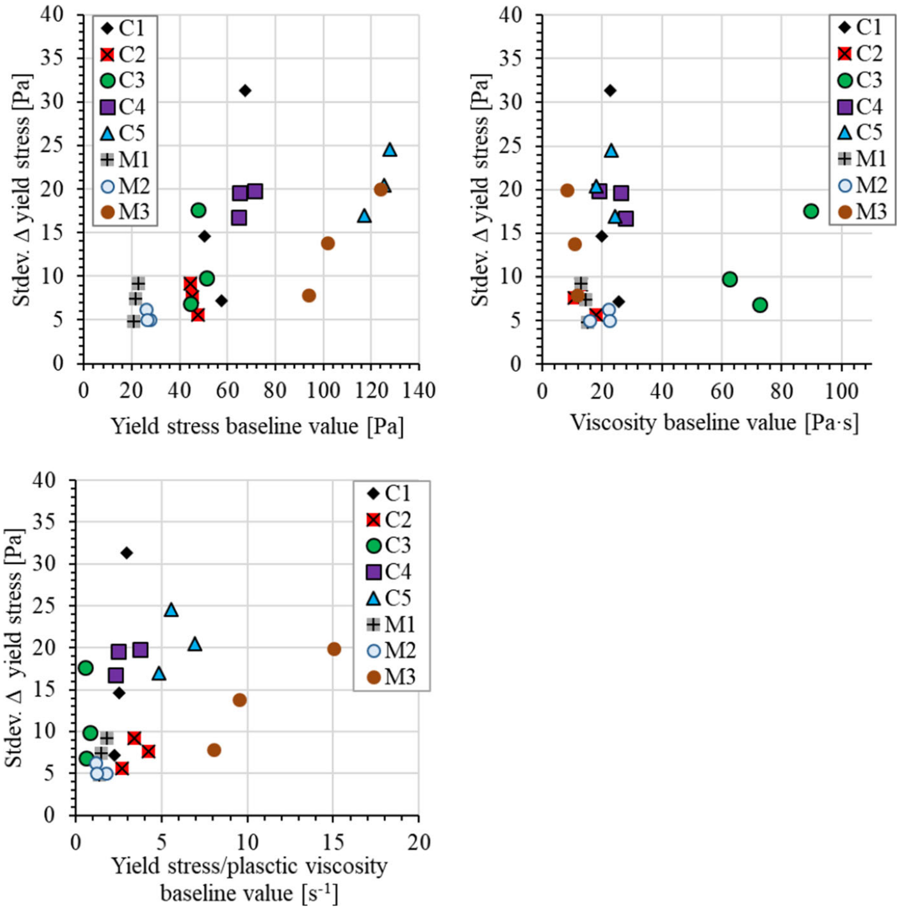

Fig. 7 Standard deviation of Δ yield stress as a function of yield stress (left), viscosity (right), or yield stress-to-viscosity ratio (bottom) separated for each test

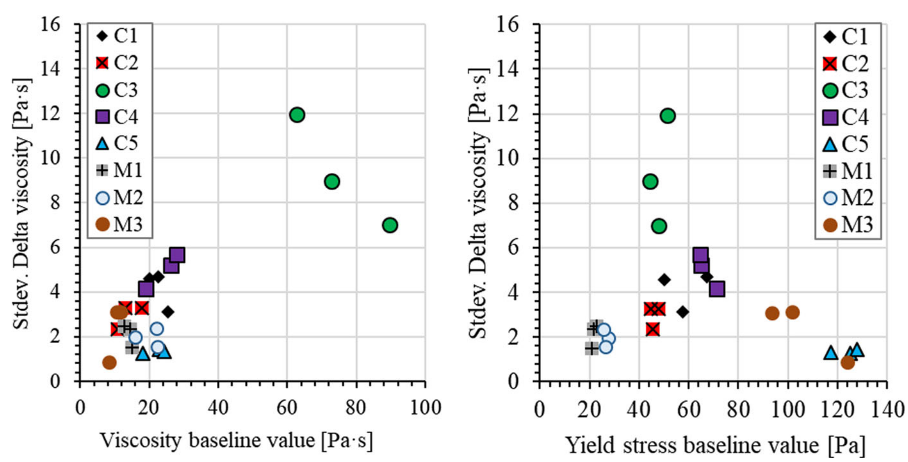

Fig. 8 Standard deviation of Δ viscosity as a function of viscosity (left) or yield stress (right), separated for each test

homogeneity, which could render the experiment less reliable. The yield stress-to-viscosity ratio explains thus the larger scatter on M3, compared to other mortar mixtures. It could to some extent also explain the difference between C1–C3 on the one hand, and C4–C5 on the other. However, when comparing C2 and C4, those two mixtures show very similar yield stress-to-viscosity ratio. On the other side, C4 shows about double the scatter compared to C2. The difference between C4–C5 and the other mixtures should thus have a second cause since they have a larger coarse aggregate volume compared to the other concrete mixtures. As such, increasing coarse aggregate content, which induces additional friction and/or non-homogeneities, is expected to be an important factor affecting the accuracy of yield stress measurements. Therefore, the presence of plug flow and coarse aggregate content might hinder a reliable measurement of the rheological properties of conventional concrete.

For viscosity, as can be seen in Fig. 8, these theories do not apply to the obtained results. There seems to be a strong correlation between the scatter on viscosity and the viscosity itself, and no correlation with either yield stress or aggregate content. It also seems that the mortars show approximately the same scatter as the concrete mixtures.

5.4 Effect of extended measuring duration

The testing procedure for ICAR 4 consisted of a significantly longer pre-shear period, i.e. 60 s instead of 20 s for concrete mixtures or 30 s for mortar, and the duration of the measuring steps was doubled as well. As mentioned in the introduction, shear-induced particle migration is an event which needs time to manifest, but the measuring duration may be sufficiently long to see its effect. If shear-induced particle migration would have the same effect on mortar as on concrete, the results for ICAR 4 would just show a lower slope compared to the baseline. However, if the measurement is sufficiently short to prevent significant particle migration of sand particles but too long to prevent it for coarse aggregates, a distinctively different result should be seen for mortar and concrete.

Figure 9 shows the relationships between the rheometer values for ICAR 3 and ICAR 4, as a function of the baseline values, for viscosity. In contrast to Figs. 1 and 2, the results of concrete and mortar are plotted separately. The relationships between mortar and concrete for ICAR 3 show similar slopes of the lines. The trendline for concrete is slightly above the trendline for mortars. For ICAR 4 though, there is a significant difference between the mortar and concrete results. Mortar viscosity values measured with ICAR 4 are in the same range as for ICAR 3. However, concrete viscosity values for ICAR 4 are substantially lower than for ICAR 3. Furthermore, the slope of the trendline for concrete measured with ICAR 4 is half of the mortar trendline with the same rheometer. These results indicate that significant particle migration may have happened during the extended procedure with ICAR 4. The results do not, however, exclude that it was not observed with ICAR 3, but the effect, if present, would be less extensive. The yield stress results did not show a significant influence.

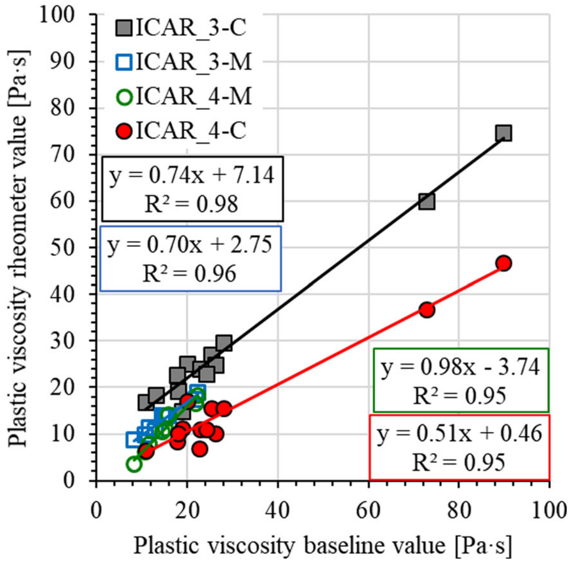

Fig. 9 Viscosity of ICAR 3 and ICAR 4 as a function of the baseline value, with the data split for concrete and mortar plotted separately

6 Conclusions

A comprehensive testing campaign of mortar and concrete mixtures was conducted in May 2018 at the Universite d'Artois in Bethune, France to compare the rheological properties of different commercially available mortar and concrete rheometers. A part of this testing campaign was dedicated to comparing the flow curve results. The selected rheometers that delivered data in fundamental units were the ICAR rheometer (four devices were used), the eBT-V, Viskomat XL and the RheoCAD with vane configuration.

With multiple weight factors, based on the number of tests executed for each rheometer, for each mixture testing time and the spread on the data, combined with an outlier analysis, a baseline value was established to compare the different rheometers.

Comparing the trendlines of the separate rheometers with the baseline reveals approximately a factor 2 spread on the readings of yield stress and viscosity. Partially, large differences could be observed. Even using the rheometers of the same type does not guarantee that the results will be comparable. However, the device-specific trendlines have strong correlations ($R^2 \geq 0.83$ for yield stress and ≥ 0.95 for viscosity) with the overall baseline. Large differences can be observed, but all trendlines have significant correlations with the baseline. Differences could be attributed to imprecisions in registering torque or velocity, or in calibration.

An analysis was also performed on the spread of the data along the trendline. This spread indicates that the tested rheometers' sensitivity is approximately constant amongst all employed devices. The results also indicate that more spread in sensitivity can be found for different mix designs than for the rheometers. The spread for yield stress is related to the presence of plug flow and an increase in coarse aggregate content, making the measurement more susceptible to errors. For viscosity, the larger the viscosity, the larger the potential error. Based on this analysis the measurement of fundamental rheological units is more reliable for flowable mixtures.

In addition, the effect of an extended measuring procedure was shown from two rheometers of the same type. Results on viscosity indicate a significant difference in the relationship between this rheometer's results for concrete and mortar when comparing to the baseline. These results indicate that significant shear-induced particle migration may have occurred in the concrete, reducing the viscosity for the longer measurement.

Acknowledgements The authors recognize the help of the scientific and technical team at the University Artois, LGCgE Laboratoire de Génie Civil et Géo-Environnement. The authors are very grateful to Mr. Faber Fabbris from concrete producer EQIOM for planning and providing "just in time" the mortar and concrete mixtures. Finally, the authors are thankful to all other participants of the Round-Robin tests: Mohammed Sonebi, Sofiane Amziane, Chafika Djelal, Faber Fabbris, Shirin Fataei, Markus Greim, Irina Ivanova, Kamal Khayat, Laurent Libessart, Viktor Mechtcherine, Ivan Navarrete, and Arnaud Perrot and their organisations for the involvement in the execution and evaluation of the Round-Robin tests.

Author contribution This document is the result of an experimental campaign supported by and carried out by a taskgroup of RILEM TC 266-MRP. Other members of the taskgroup who contributed to the experimental campaign and the data treatment are: MS, SA, CD, SF, MG, II, KK, LL, VM, IN, and AP. Other members of RILEM TC 266-MRP, not involved in the taskgroup are: RC, GDS, SF, SG, MH, SJ, KL, JL, DL, TP, NR, WS, JV, JEW, AY, and JZ. This paper was reviewed and approved by all members of the committee.

Declarations

Conflict of interest None of the authors declare a conflict of interest.

References

1. Feys D, Sonebi M, Amziane S, Djelal C, El Cheikh K, Fabbris F, Fataei S, Greim M, Ivanova I, Keller H, Khayat K, Libessart L, Mechcherine V, Navarrete I, Perrot A, Secrieru E, Vanhove Y (2023) RILEM TC 266-MRP: round-robin rheological tests on high performance mortar and concrete with adapted rheology—rheometers, mixtures and procedures, Mater Struct 56:90
2. Banfill P, Beaupré D, Chapdelaine F, de Larrard F, Domone P, Nachbaur L, Sedran T, Wallevik O, Wallevik JE (2000) Comparison of concrete rheometers: international tests at LCPC (Nantes, France), Nantes
3. Ferraris CF, Brower LE, Beaupré D, Chapdelaine F, Struble L, Domone P, Koehler E, Lin S, Sonebi M, Struble L, Tepke D, Wallevik O, Wallevik JE (2004) Comparison of concrete rheometers: international tests at MB. Cleveland OH, USA
4. Haist M, Link J, Nicia D, Leinitz S, Baumert C, von Bronk T, Cotardo D, Eslami Pirharati M, Fataei S, Garrecht H, Gehlen C, Hauschildt I, Ivanova I, Jesinghausen S, Klein C, Krauss H-W, Lohaus L, Lowke D, Mazanec O, Pawelczyk S, Pott U, Radebe NW, Riedmiller JJ, Schmid H-J, Schmidt W, Secrieru E, Stephan D, Thiedeitz M, Wilhelm M, Mechtcherine V (2020) Interlaboratory study on rheological properties of cement pastes and reference substances: comparability of measurements performed with different rheometers and measurement geometries. Mater Struct 53:92
5. Tattersall GH, Banfill PFG (1983) The rheology of fresh concrete. Pitman Books Ltd., London
6. Wallevik JE (2003) Rheology of particle suspensions. Fresh concrete, mortar and cement paste with various types of

lignosulfonates, The Norwegian university of science and technology (NTNU)
7. Wallevik ÓH, Wallevik JE (2011) Rheology as a tool in concrete science: The use of rheographs and workability boxes. Cem Concr Res 41:1279–1288
8. Ferraris CF, Martys NS, Concrete rheometers, In: Roussel N (Ed), Underst Rheol Concr, 1st ed., Woodhead Publishing Limited, 2012: pp. 63–82.
9. Roussel N (2006) A thixotropy model for fresh fluid concretes: theory, validation and applications. Cem Concr Res 36:1797–1806
10. Wallevik OH, Feys D, Wallevik JE, Khayat KH (2015) Avoiding inaccurate interpretations of rheological measurements for cement-based materials. Cem Concr Res 78:100–109
11. Feys D, Khayat KH (2017) Particle migration during concrete rheometry: How bad is it? Mater Struct 50:122
12. Baumert C, Garrecht H (2020) Minimization of the influence of shear-induced particle migration in determining the rheological characteristics of self-compacting mortars and concretes. Materials (Basel) 13:1542
13. Roussel N, Ovarlez G, Garrault S, Brumaud C (2012) The origins of thixotropy of fresh cement pastes. Cem Concr Res 42:148–157
14. Feys D, Cepuritis R, Jacobsen S, Lesage K, Secrieru E, Yahia A (2017) Measuring rheological properties of cement pastes: most common techniques, procedures and challenges. RILEM Tech Lett 2:129–135
15. Ley-Hernández AM, Feys D, Kumar A (2020) How do different testing procedures affect the rheological properties of cement paste? Cem Concr Res 137:106189
16. Feys D, Verhoeven R, De Schutter G (2009) Why is fresh self-compacting concrete shear thickening? Cem Concr Res 39:510–523
17. Zhu H, Martys NS, Ferraris C, De Kee D (2010) A numerical study of the flow of bingham-like fluids in two-dimensional vane and cylinder rheometers using a smoothed particle hydrodynamics (SPH) based method. J Nonnewton Fluid Mech 165:362–375
18. Rabia A, Yahiaoui S, Djabourov M, Feuillebois F, Lasuye T (2014) Optimization of the vane geometry. Rheol Acta 42:357–371
19. Wallevik JE (2008) Minimizing end-effects in the coaxial cylinders viscometer: viscoplastic flow inside the ConTec BML viscometer 3. J Nonnewton Fluid Mech 155:116–123
20. Spangenberg J, Roussel N, Hattel JH, Stang H, Skocek J, Geiker MR (2012) Flow induced particle migration in fresh concrete: theoretical frame, numerical simulations and experimental results on model fluids. Cem Concr Res 42:633–641
21. Spangenberg J, Roussel N, Hattel JH, Sarmiento EV, Zirgulis G, Geiker MR (2012) Patterns of gravity induced aggregate migration during casting of fluid concretes. Cem Concr Res 42:1571–1578
22. Wallevik JE (2014) Effect of the hydrodynamic pressure on shaft torque for a 4-blades vane rheometer. Int J Heat Fluid Flow 50:95–102